Electronic Supplementary Material (ESI) for Soft Matter.

Electronic Supplementary Information

Table of Contents

18 June, 2022

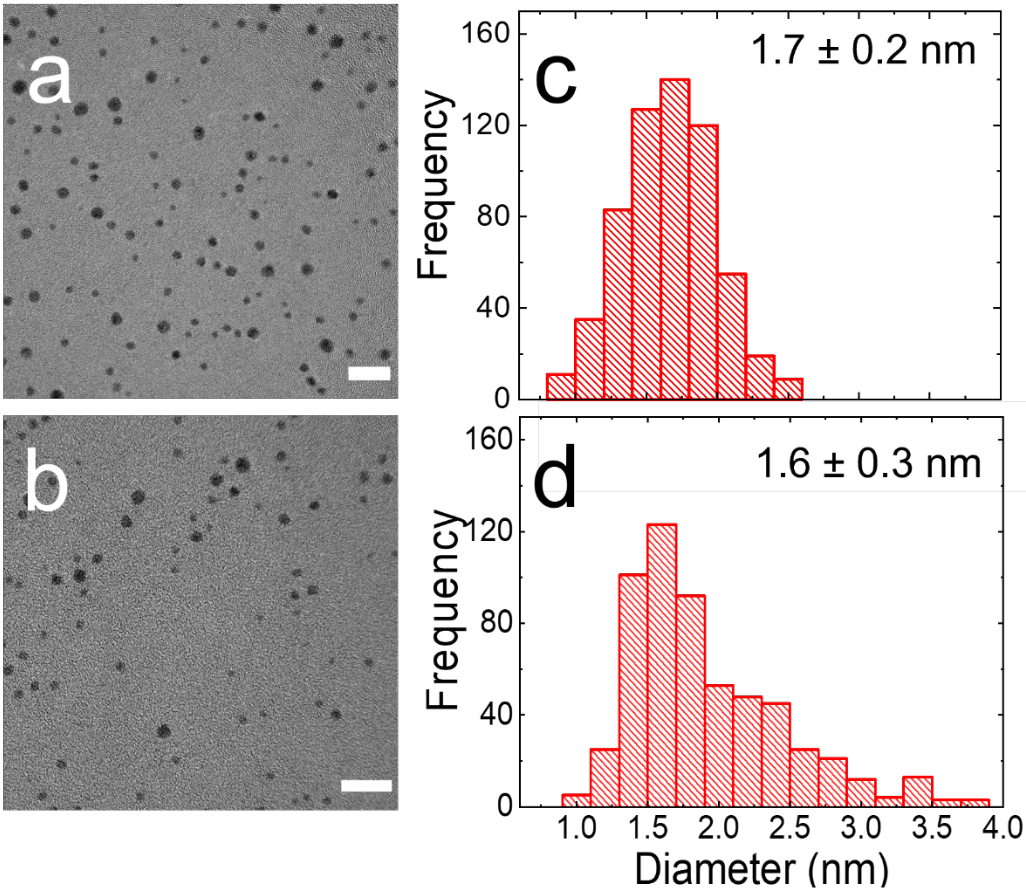

Figure S1. TEM micrographs and size-distribution histograms for as-prepared (a,c) G6-NH_2(Au_{147}) DENs and (b,d) G6-OH(Au_{147}) DENs. TEM grids for size analysis were prepared by dropcasting 2 µL of Au DEN solution onto a continuous carbon-coated, 400 mesh Cu TEM grid and drying in air. Size distributions were determined by analyzing a total of 200 NPs from each of three independently prepared grids. The scale bar is 10 nm.

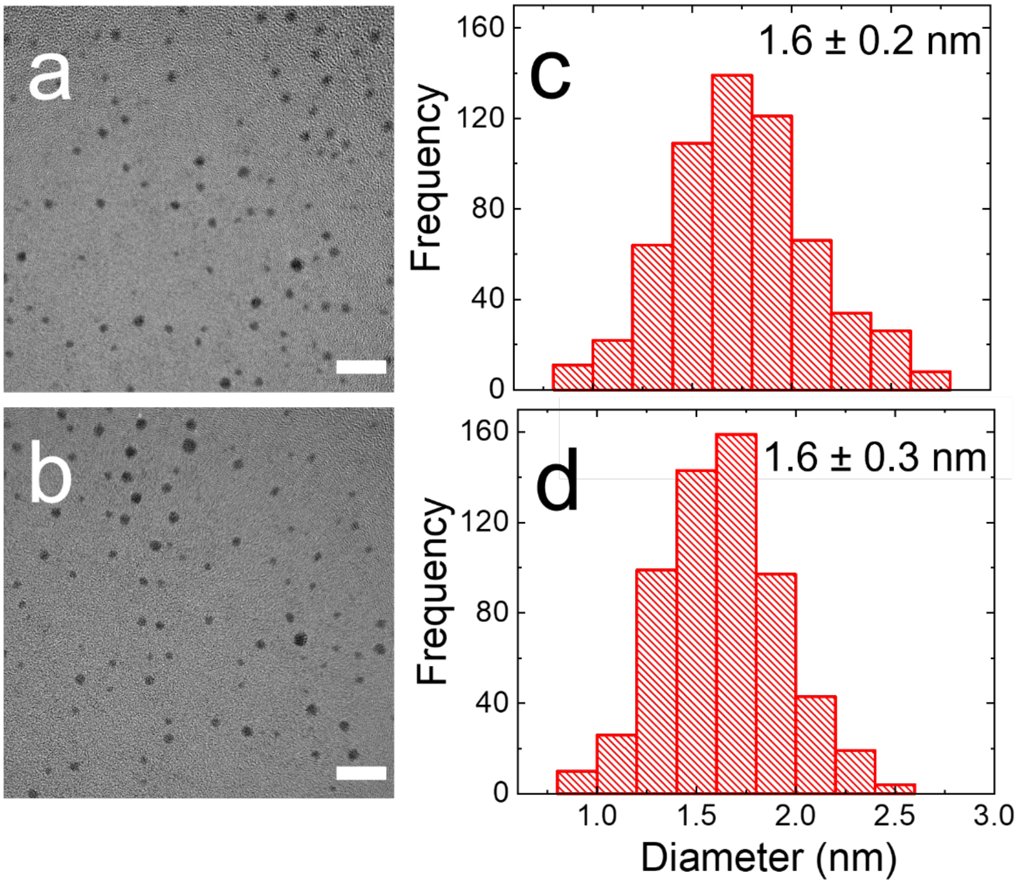

Figure S2. TEM micrographs and size-distribution histograms for (a,c) once-dialyzed G6-NH$_2$(Au$_{147}$) DENs and (b,d) twice-dialyzed G6-NH$_2$(Au$_{147}$) DENs. TEM grids for size analysis were prepared by dropcasting 2 µL of Au DEN solution onto a continuous carbon-coated, 400 mesh Cu TEM grid and drying in air. Size distributions were determined by analyzing a total of 200 NPs from each of three independently prepared grids. The scale bar is 10 nm.

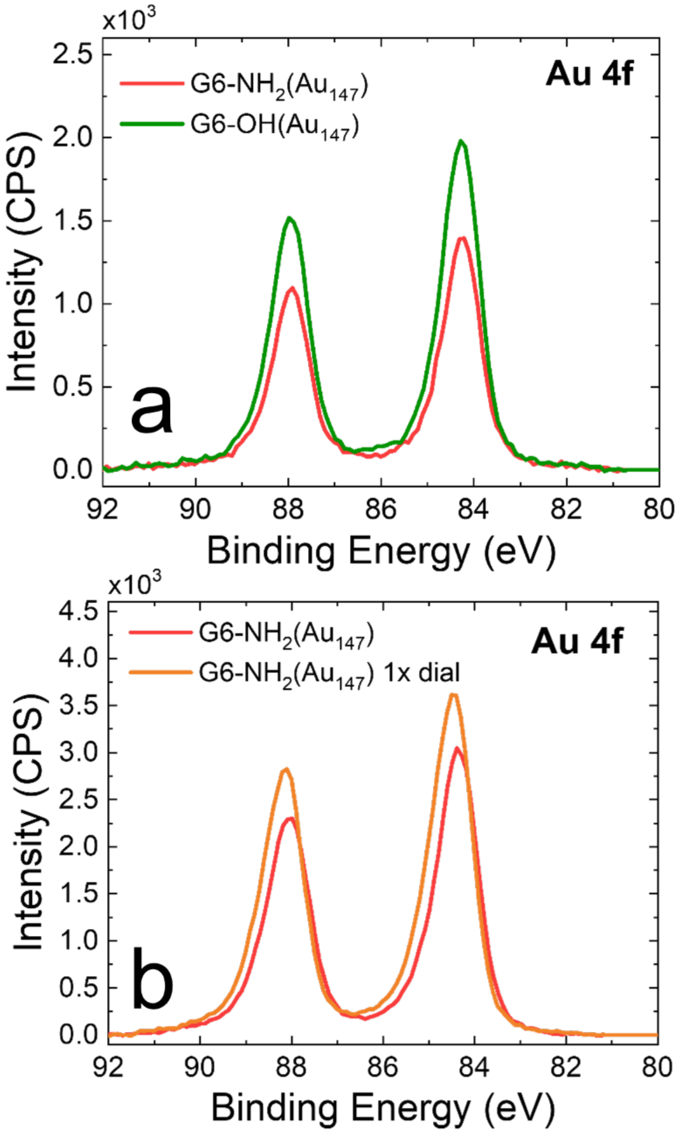

Figure S3. XPS spectra in the Au 4f region of (a) as-prepared G6-NH_2(Au_{147}) and G6-OH(Au_{147}) DENs and (b) as-prepared and dialyzed G6-NH_2(Au_{147}) DENs. Samples for XPS experiments were prepared by dropcasting 2 μL of an Au DEN solution onto a continuous carbon-coated, 400 mesh Cu TEM grid and drying in air. Prior to XPS analysis, samples were grounded using carbon tape. XPS measurements were carried out using a Kratos Axis Ultra DLD spectrometer (Chestnut Ridge, NY). Spectra were collected using an Al Kα source, 0.10 eV step size, and 20 eV band pass energy. Binding energies (BE) were calibrated using the C 1s line (284.5 eV).[1,2]

For as-prepared G6-NH_2(Au_{147}) and G6-OH(Au_{147}) DENs, the two Au 4f peaks are present at 87.9 eV (Au $4f_{5/2}$) and 84.2 eV (Au $4f_{7/2}$). These values are consistent with the reported BEs for zerovalent Au and G6-NH_2(Au_{147}) DENs.[1,2] A small increase in the Au 4f BEs for G6-NH_2(Au_{147}) DENs is observed following dialysis. This change is likely caused by slight oxidation of the Au NP surface during dialysis.[1] The XPS results indicate that there is no significant difference in oxidation state between Au DEN samples.[3,4] We conclude that the SA/SCs are zerovalent Au stabilized by dendrimers and not ionic forms of gold stabilized by ligands such as Cl^-.

Section S1. To quantify the SA/SC distributions in Au or Pd DENs, the Au or Pd EDS signal was collected from selected areas of the TEM grid. The red box in **Figure 1a** of the main text is representative of such an area. These selected areas were at least 5 nm away from the edge of NPs to minimize signal arising from the NPs and SAs/SCs within the dendrimer (represented by the 8 nm circle in **Figure 1a**). Note that for grids containing undialyzed G6-$NH_2(Au_{147})$ DENs there are a significant number of SAs/SCs at least 5 nm from the NPs, which are not observed in the other Au or Pd DEN samples.

EDS spectra were collected and analyzed using the Pathfinder software package from ThermoFisher Scientific. TEM grids for EDS analysis were prepared by dropcasting 2 μL of either Au or Pd DEN solution onto a SiO_2-coated, 400 mesh Cu TEM grid and drying in air or N_2, respectively.

EDS spectra for Au and Pd DENs were measured in an energy range from 0 to 80 keV. The Si EDS signal from the underlying SiO_2 support coating of the Cu TEM grid was collected concurrently with the Au and Pd EDS signals and used for normalization to account for variations in EDS scan area and time.

The Au EDS signal is the sum of the net counts from the Au L (9.71 keV) and M (2.12 keV) X-ray lines. The normalized net counts were calculated by dividing the Au net counts by the Si net counts obtained at the Si K line (1.74 keV).

The Pd EDS signal is the sum of the net counts from the Pd L (2.84 keV) and K (21.18 keV) X-ray lines. Normalization was performed using the same method as for the Au net counts.

Table S1. Average values for the Au EDS signals in **Figure 2** of the main text. The error bars represent the standard deviation from the mean for Au EDS signals obtained from 10 EDS spectra collected within one grid square.

	Normalized net counts (Au/Si)
G6-NH_2(Au_{147}) as prepared	1.0 ± 0.4
G6-NH_2(Au_{147}) dialyzed 1x	0.15 ± 0.09
G6-NH_2(Au_{147}) dialyzed 2x	0.1 ± 0.2
G6-OH(Au_{147})	0.10 ± 0.08
Blank grid	0.05 ± 0.05

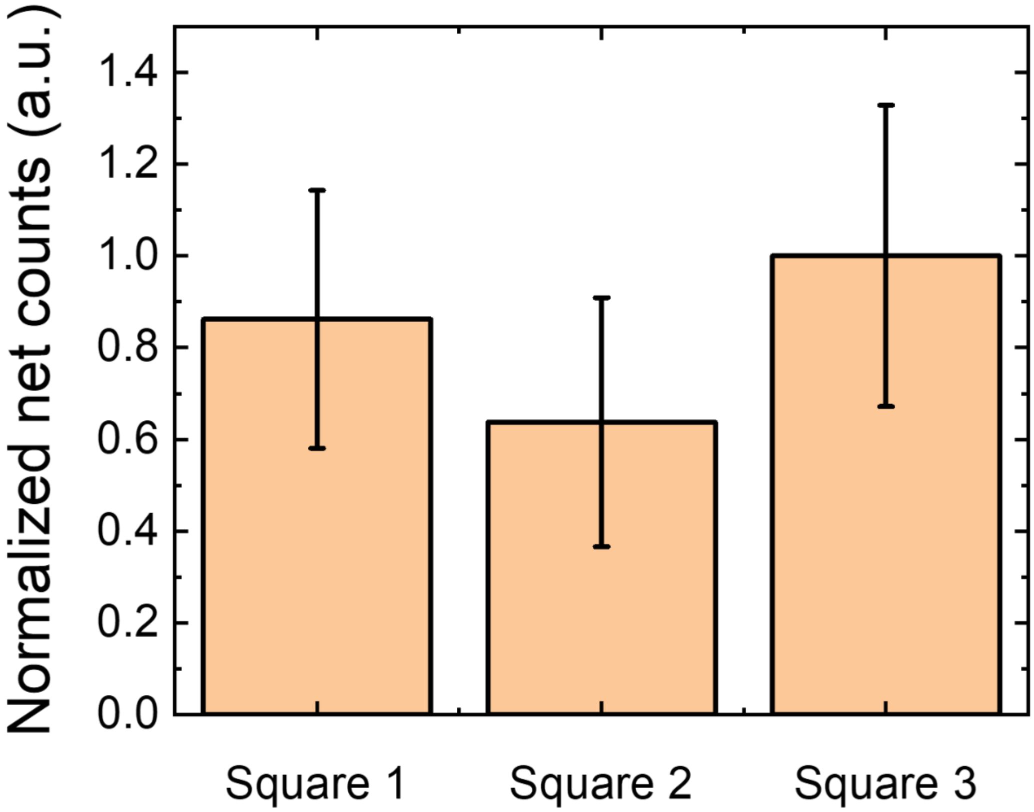

Figure S4. Histogram showing the Si EDS signals from a SiO_2-coated, 400 mesh Cu TEM grid. For this sample, EDS spectra were collected from three different grid squares on the same TEM grid. The Si net counts were normalized by the number of frames and scan area. The error bars represent the standard deviation from the mean for Si EDS signals obtained from 10 EDS spectra collected within one grid square. These data show that the Si EDS signal is, within error, uniform in different locations on the same TEM grid.

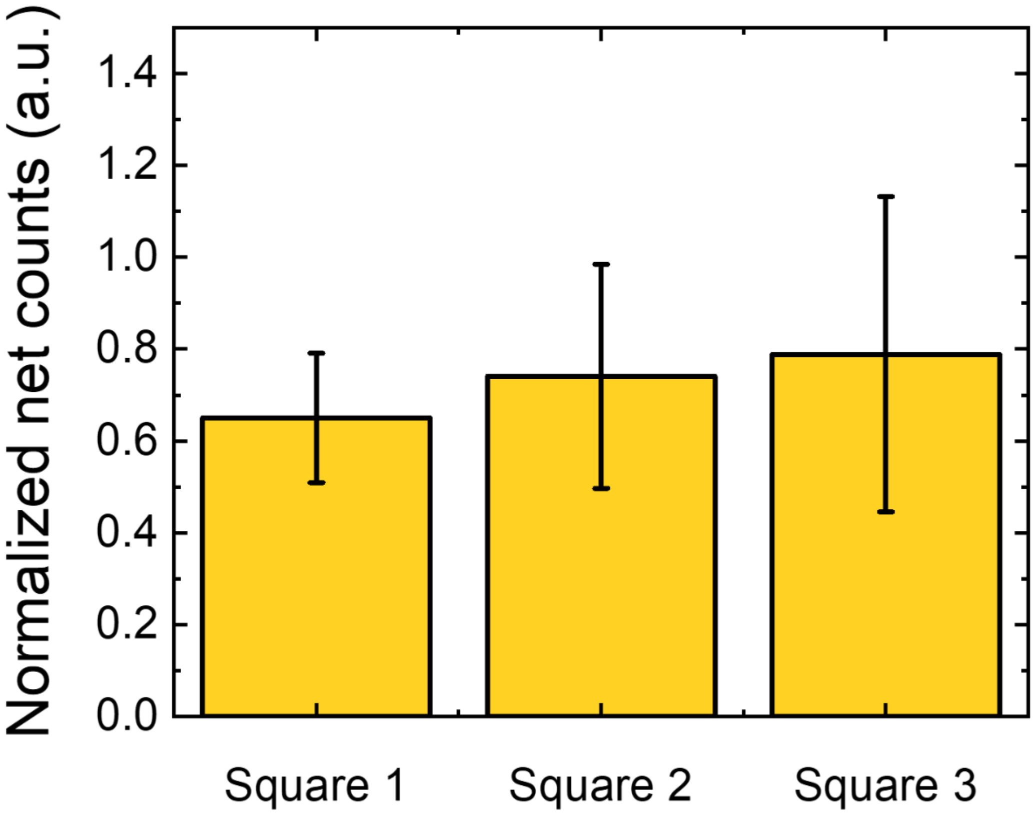

Figure S5. Histogram showing the Au EDS signals from an as-prepared G6-$NH_2(Au_{147})$ DEN sample. For this case, EDS spectra were collected from three different grid squares on the same TEM grid. The error bars represent the standard deviation from the mean for Au EDS signals obtained from 10 EDS spectra collected within one grid square. These data show that the Au EDS signal is, within error, uniform in different locations on the same TEM grid. TEM grids for EDS analysis were prepared by dropcasting 2 μL of Au DEN solution onto a SiO_2-coated, 400 mesh Cu TEM grid and drying in air.

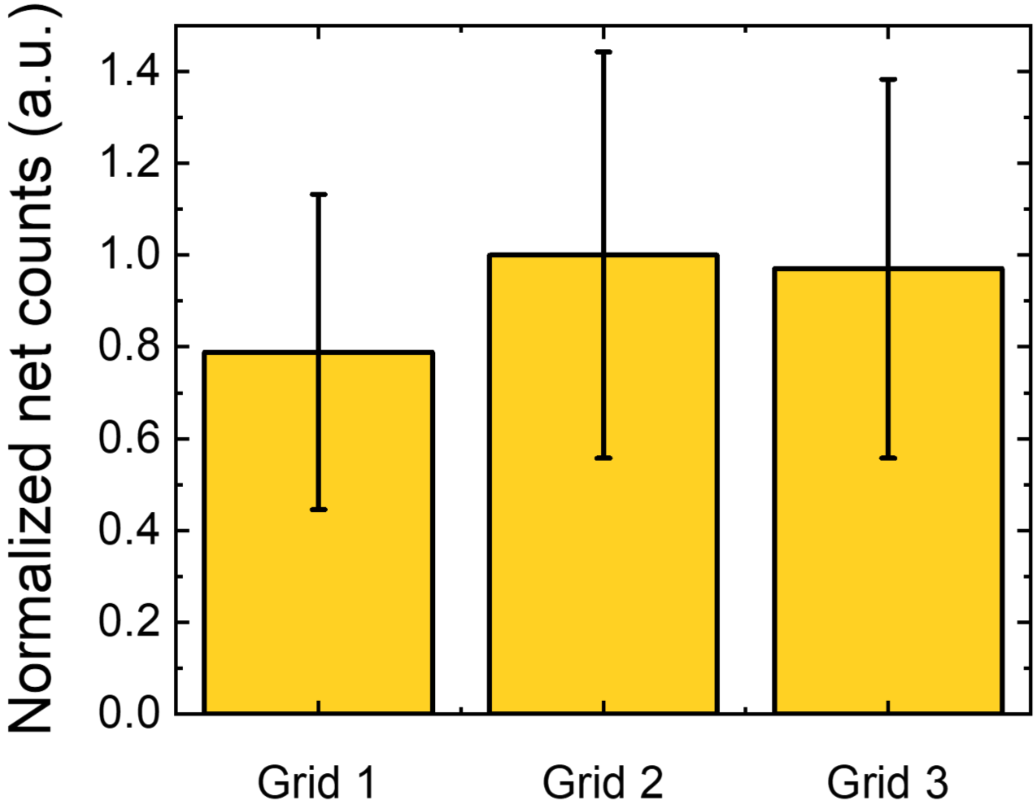

Figure S6. Histogram showing the Au EDS signals from as-prepared G6-$NH_2(Au_{147})$ DEN samples. For this analysis, EDS spectra were collected from one grid square on each of three independently prepared TEM grids. The error bars represent the standard deviation from the mean for Au EDS signals obtained from 10 EDS spectra collected within one grid square. These data show that the Au EDS signal is, within error, uniform between independently prepared TEM grids. TEM grids for EDS analysis were prepared by dropcasting 2 µL of Au DEN solution onto a SiO_2-coated, 400 mesh Cu TEM grid and drying in air.

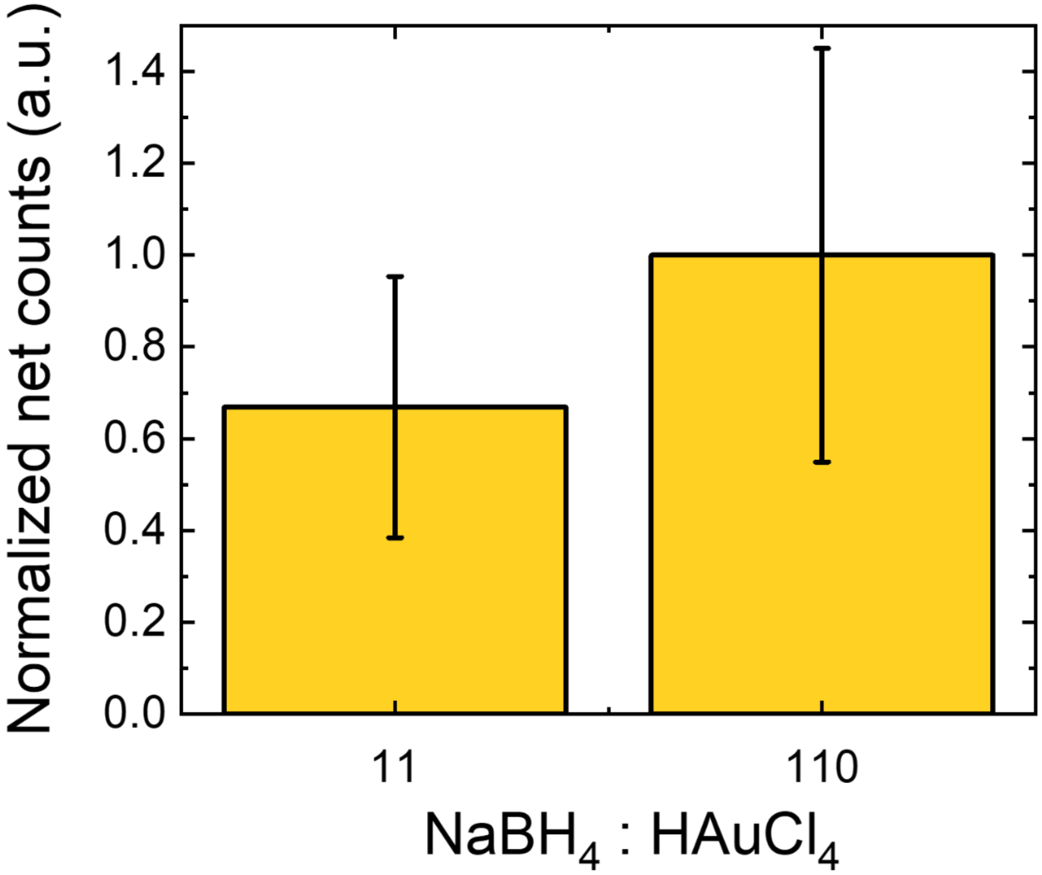

Figure S7. Histogram showing the Au EDS signal obtained from G6-NH$_2$(Au$_{147}$) DENs prepared using either an 11- or 110-fold excess of NaBH$_4$. The error bars represent the standard deviation from the mean for Au EDS signals obtained from 10 EDS spectra collected within one grid square. These data show that increasing the equivalents of NaBH$_4$ does not significantly change the Au EDS signal. TEM grids for EDS analysis were prepared by dropcasting 2 μL of Au DEN solution onto a SiO$_2$-coated, 400 mesh Cu TEM grid and drying in air.

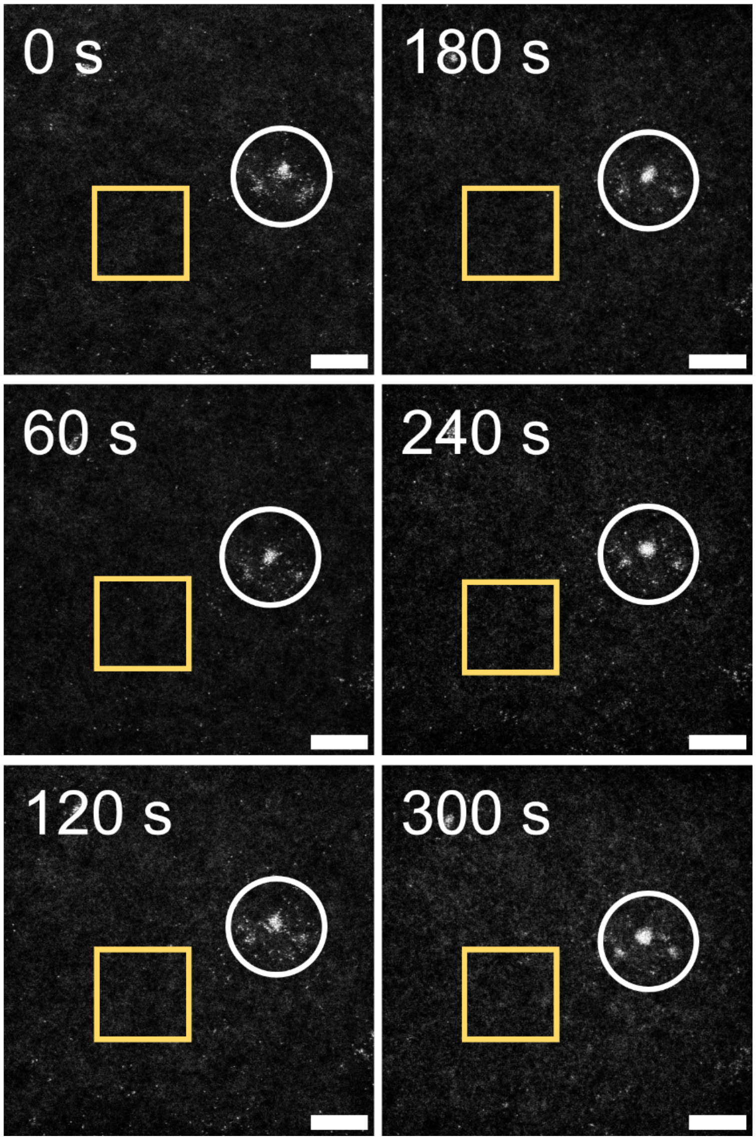

Figure S8. A series of ac-STEM micrographs obtained from a single area of a grid containing twice-dialyzed G6-$NH_2(Au_{147})$ DENs. This area of the grid was not exposed to the electron beam prior to image acquisition. Images were captured every 60 s over a 5 min period of constant beam exposure. The 8 nm circle represents the approximate location of the dendrimer encapsulating the central, largest NP. EDS data were collected from the region represented by the yellow box. The edge of the yellow box is ~10 nm away from the edge of the largest DEN and ~5 nm away from the leftmost clusters. Although some atom movement and carbon build-up occur over the 5 min exposure period, the number of SAs/SCs contained within the yellow box did not increase significantly. This result indicates that the majority of SAs/SCs within the box are not generated due to damage to the NPs during electron beam exposure. TEM grids for ac-STEM analysis were prepared by dropcasting 2 μL of Au DEN solution onto a continuous carbon-coated, 400 mesh Cu TEM grid and drying in air. The scale bar is 5 nm.

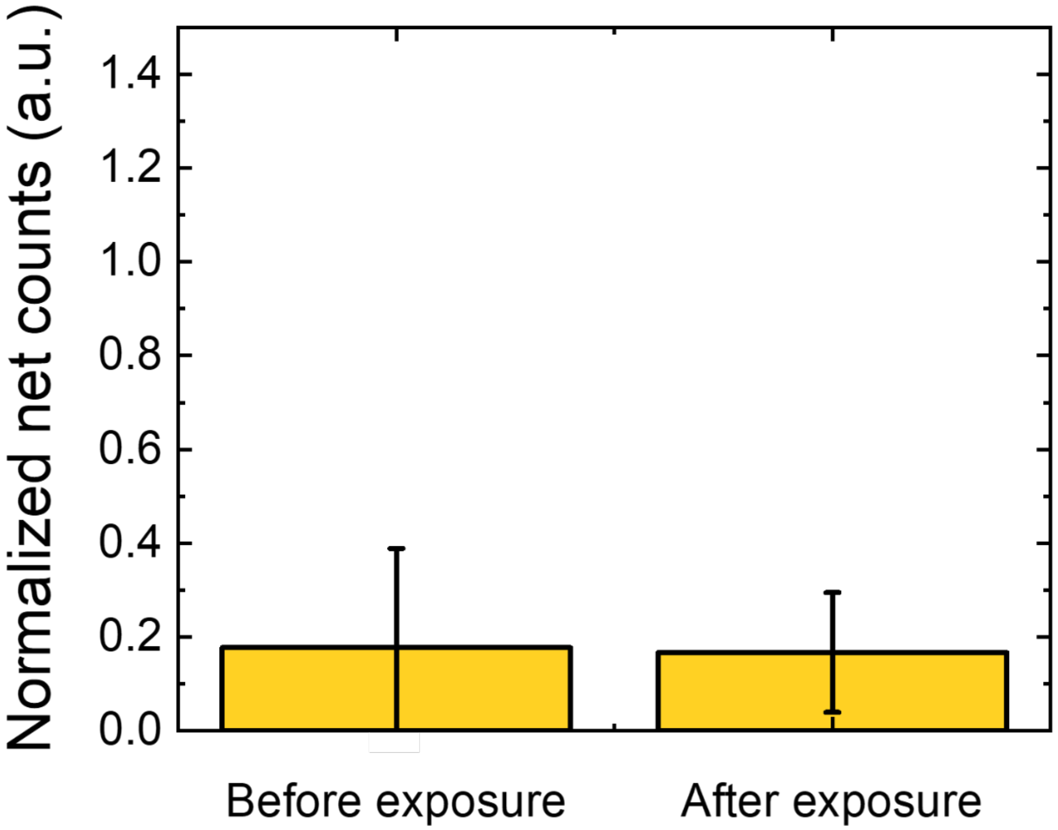

Figure S9. Histogram showing the Au EDS signal from a twice-dialyzed G6-$NH_2(Au_{147})$ DEN sample. For this sample, EDS spectra were collected from a single selected grid area, similar to the yellow box in **Figure S8**, both before and after a 5 min period of continuous electron beam exposure. The error bars represent the standard deviation from the mean for Au EDS signals obtained from 10 consecutive EDS spectra collected in the selected grid area. These data show that continuous electron beam exposure does not significantly change the Au EDS signal collected in a selected grid area. TEM grids for EDS analysis were prepared by dropcasting 2 μL of Au DEN solution onto a SiO_2-coated, 400 mesh Cu TEM grid and drying in air.

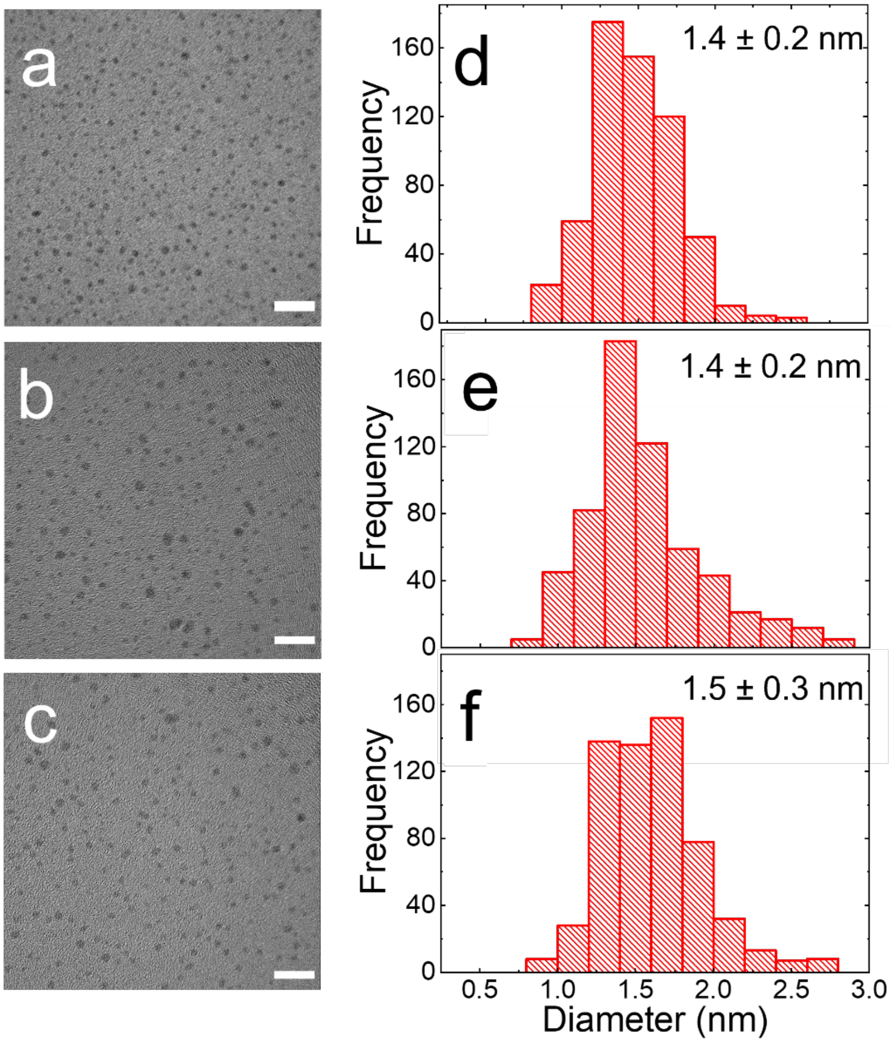

Figure S10. TEM micrographs and size-distribution histograms for (a,d) as-prepared G6-OH(Pd_{147}) DENs, (b,e) dialyzed G6-OH(Pd_{147}) DENs, and (c,f) as-prepared G6-NH_2(Pd_{147}) DENs. TEM grids for size analysis were prepared by dropcasting 2 μL of Pd DEN solution onto a continuous carbon-coated, 400 mesh Cu TEM grid and drying under N_2. Size distributions were determined by analyzing a total of 200 NPs from each of three independently prepared grids. The scale bar is 10 nm.

Table S2. Average values for the Pd EDS signals used for **Figure 4** in the main text. The error bars represent the standard deviation from the mean for Pd EDS signals obtained from 10 EDS spectra collected within one grid square.

	Normalized net counts (Pd/Si)
G6-OH(Pd_{147}) as prepared	0.15 ± 0.09
G6-OH(Pd_{147}) dialyzed 1x	0.1 ± 0.2
G6-NH_2(Pd_{147}) as prepared	0.07 ± 0.05
Blank grid	0.05 ± 0.05

References

1 NIST X-ray Photoelectron Spectroscopy (XPS) Database, Version 4.1, https://srdata.nist.gov/xps/Default.aspx, (accessed 16 June 2022).

2 A. Galyamova, K. Shin, G. Henkelman and R. M. Crooks, *J. Phys. Chem. C*, 2020, **124**, 10045–10056.

3 Gold – XPS Analysis - Cardiff University, http://sites.cardiff.ac.uk/xpsaccess/reference/gold/, (accessed 16 June 2022).

4 Z. Chen, Y. Chen, S. Chao, X. Dong, W. Chen, J. Luo, C. Liu, D. Wang, C. Chen, W. Li, J. Li and Y. Li, *ACS Catal.*, 2020, **10**, 1865–1870.